



Valorization of forest by-products as bio-adsorbents for emerging contaminants

Lucía Rodríguez-López^{a,b,*}, Vanesa Santás-Miguel^{a,b}, Raquel Cela-Dablanca^c, Paula Pérez-Rodríguez^{a,b}, Avelino Núñez-Delgado^c, Esperanza Álvarez-Rodríguez^c, Andrés Rodríguez-Seijo^{a,b}, Manuel Arias-Estévez^{a,b}

^a Department of Plant Biology and Soil Science, Area of Soil Science and Agricultural Chemistry, Faculty of Sciences, University of Vigo, Ourense 32004, Spain

^b Agroecology and Food Institute (IAA), University of Vigo – Campus Atuga, 32004 Ourense, Spain

^c Dept. Soil Science and Agricultural Chemistry, Engineering Polytechnic School, University of Santiago de Compostela, 27002 Lugo, Spain

ARTICLE INFO

Editor: Zacharias Frontistis

Keywords:

Retention
Liberation
Pharmaceuticals
Circular economy
Environmental remediation
pH

ABSTRACT

The use of forest by-products as bio-adsorbents allows the recycling of these materials and could reduce the risks of environmental pollution due to different contaminants. This study focuses on the adsorption and release of three antibiotics (ciprofloxacin, clarithromycin and trimethoprim) on pine and oak bark materials and how pH influences in these processes. The results showed that the highest adsorption potential corresponds to pine bark, where the Freundlich affinity coefficient varies between 126.6 and 2979.1 Lⁿ μmol¹⁻ⁿ kg⁻¹, while, for oak bark, between 283.9 and 806.9 Lⁿ μmol¹⁻ⁿ kg⁻¹. Both bio-adsorbents show some influence of the pH affecting adsorption. Of the three antibiotics, clarithromycin was the most mobile. In general, both by-products gave satisfactory results as bio-adsorbents for the antibiotics tested. Therefore, their potential use as decontaminants could help to face environmental issues due to these emerging pollutants, reducing human and ecological risk, while contributing to a zero-waste economy.

1. Introduction

Soil and water pollution due to antibiotics are serious environmental issues. These emerging contaminants reach soils and water bodies through irrigation with effluents from wastewater treatment plants, as well as through the application of sewage sludge as fertilizers, and also by spreading manure and slurry in the case of veterinary antibiotics [1]. Depending on the treatment used in wastewater treatment plants, these contaminants are not completely eliminated [2,3], and then reach soils, where they may favour the appearance and propagation of antibiotic resistance genes. The evolution of these compounds, once they reach the soil, will vary depending on different chemical and biological processes (adsorption-desorption, degradation, transport), and they could pass to other environmental compartments [1,2], and thus both the compounds and the resistance genes could enter the food chain, affecting animals and human beings, generally favouring microbial resistance to these biocides. Numerous studies demonstrate the presence of these genes in agricultural soils [4], crops [3] and waterbodies [5].

One alternative to retain them and prevent their mobilization to other environmental compartments is the application of different bio-adsorbents, increasing the adsorption capacity of soils and avoiding their transport to waterbodies. The technique of using bio-adsorbents is simple, low cost and easy to carry out, increasing the specific surface area and the adsorption capacity for antibiotics [6]. Multiple studies can be found regarding a variety of materials, including residues or by-products, for the retention of different contaminants. Among them are biochar [7,8], shells of different animals [9,10], activated carbon [11] or by-products from different foods, such as rice husks [12] or nuts [13]. The application of bio-adsorbents, in addition to facilitating the adsorption of contaminants, makes it possible to recycle residues or by-products, and thus contribute to a circular economy. Its use is widespread for multiple contaminants, such as heavy metals [13–15], pesticides [16,17], herbicides [18–20], and polycyclic aromatic hydrocarbons (PAHs) [21], among others.

Within bio-adsorbents, various by-products from the forestry industry can be seen as relevant, with tree bark being among the most

* Corresponding author at: Department of Plant Biology and Soil Science, Area of Soil Science and Agricultural Chemistry, Faculty of Sciences, University of Vigo, Ourense 32004, Spain.

E-mail address: lucia.rodriguez.lopez@uvigo.gal (L. Rodríguez-López).

<https://doi.org/10.1016/j.jece.2023.111437>

Received 5 July 2023; Received in revised form 21 October 2023; Accepted 6 November 2023

Available online 8 November 2023

2213-3437/© 2023 The Author(s). Published by Elsevier Ltd. This is an open access article under the CC BY-NC-ND license (<http://creativecommons.org/licenses/by-nc-nd/4.0/>).

abundant. Europe is the continent placed second in wood production (31.9% of world production in 2021) after America (37.9%) [22]. Specifically, in Spain, since the 19th century, the largest reforestations were made with pine, especially *Pinus pinaster*, and between the hardwood and less pyrophilous species, the genus *Quercus* (i.e., *Q. suber*) [23].

In the case of cork oak bark, it is processed to obtain cork for the manufacture of bottle stoppers, as well as to obtain sheets to install in homes as insulation and waterproofing, among many other uses [24], generating multiple amounts of waste, including the so-called "cork dust", which is not used for the production of corks or the manufacture of agglomerates, since its particle size is inadequate. One of the main destinations of this by-product is burning to obtain energy [25]. In 2015, the annual production of cork waste in Spain was around 50,000 tons [19], and between 40% and 70% of these by-products ended up in landfills [26].

Regarding pine bark, it is generated during the felling of the trees. In fact, for the use of this wood, it is necessary to remove the bark by chipping, as well as in the lumber industries where the wood is processed, such as paper pulp factories. Therefore, it is a very abundant by-product that, although it is mainly used to obtain energy, may be associated to a major concern related to its disposal, due to the large volume generated [27]. However, it can be considered a by-product among the most used as bio-adsorbent material [28].

Despite the fact that both barks are widely used as bio-adsorbents for pollutants, no studies have been carried out focusing on their efficacy as regards the adsorption of the antibiotics ciprofloxacin, trimethoprim and clarithromycin. This would be of relevance, as clarithromycin and ciprofloxacin are the antibiotics most frequently found in wastewater effluents, both worldwide and in Spain, until values of 500 ng L⁻¹ and 9.7 µg L⁻¹, respectively [2,3]. These antibiotics belong to three of the groups most widely used in human medicine: fluoroquinolones (ciprofloxacin), macrolides (clarithromycin) and diaminopyrimidines (trimethoprim), and the fact that they are widely used is largely due to their broad-based spectrum of activity against pathogen microorganisms.

Therefore, the main objectives of this study are to determine the adsorption capacity of two bio-adsorbents (pine bark and cork oak bark) for three antibiotics [ciprofloxacin (Cip), trimethoprim (Tri) and clarithromycin (Cla)], at different concentrations, as well as the influence of the variation of pH for a fixed antibiotic concentration. Additionally, it is intended to obtain information on the release of the three antibiotics from both barks, at three different pHs. With this, the experiments would provide data about the adsorption capacity of both by-products, which could help to design procedures to avoid/reduce the mobility of the antibiotics from WWTP effluents to waterbodies or soils, as well as the possibility of achieving an effective reuse and recovery of two very abundant by-products, contributing to a circular economy.

2. Materials and methods

2.1. Analyses of the forest by-products

To carry out this research, two forest by-products were used: pine bark and cork oak bark provided by Geolia (Madrid, Spain) and Corchos Almeida S.L. (Ourense, Spain), respectively. Both oak barks used in the experiment were dried, ground and sieved and provided by the company with a particle size of less than 1 mm, mostly less than 0.20 mm, that were homogenized before being used in this investigation. Details about each bioadsorbent are given in Table S1. Besides, both by-products were characterized by infrared spectroscopy analysis (IR) (FTIR-Bomen MB102 (ABB, Switzerland)). The spectra were obtained by transmittance using KBr pellets, and the determinations were made in the region between 400 and 4000 cm⁻¹, with a resolution of 4 cm⁻¹ carried out at CACTUS (University of Santiago de Compostela, Spain). Details about each by-product are given in Figs. S1 and S2.

The pH of both bark materials was measured in water (using a 1:2.5

bio-adsorbent: solution ratio) [29]. Organic carbon as well as total nitrogen, were determined on an elemental analyzer (Thermo Finnigan 1112 Series NC, Thermo Finnigan, The Netherlands). To determine the effective cation exchange capacity (eCEC), the study extracted exchangeable basic cations (Na_e, K_e, Ca_e, and Mg_e) using 0.2 M NH₄Cl and exchangeable Al (Al_e) using 1 M KCl. The extracted cations were measured using atomic absorption flame spectrophotometry for Ca, Mg and Al, while Na and K were measured using atomic emission spectrophotometry (AAAnalyst 200 spectrophotometer, PerkinElmer, Boston, MA, USA). This process was based on methods developed by Sumner and Miller [30] for exchangeable cations and Bertsch and Bloom [31] for exchangeable Al. Phosphorus was quantified by colourimetric determination by performing the extraction with NaHCO₃ [32]. The superficial area of the barks was determined using the BET analysis, developed by Brunauer, Emmett and Teller. It was carried out in an Accelerated Surface Area and Porosimetry System equipment (Micromeritics ASAP 2020, Norcross, USA).

2.2. Chemical reagents

The antibiotics ciprofloxacin (Cip), clarithromycin (Cla) and trimethoprim (Tri) with 98% purity were supplied by Sigma-Aldrich (Barcelona, Spain). Its main characteristics are listed in Table S2. All the reagents that were used to quantify antibiotics by High-Performance Liquid Chromatography (HPLC) (acetonitrile, phosphoric acid and monopotassium phosphate), as well as the other additional reagents (sodium hydroxide, sodium chloride, hydrochloric acid) were of analytical grade, supplied by Panreac (Barcelona, Spain) and by Fisher Scientific (Madrid, Spain). All the solutions used were prepared with Milli-Q water (Millipore, Madrid, Spain).

2.3. Adsorption/desorption experiments

To carry out the batch-type adsorption experiments, the following procedures were used. In the case of Cla, 0.5 g of bark were weighed in centrifuge tubes, and then suspended in 20 mL of antibiotic solution, using seven different concentrations (between 2.5 and 100 µM). For the other two antibiotics (Cip and Tri), 0.5 g of bark were weighed and suspended in 40 mL of antibiotic (each of the two antibiotics individually) with concentrations between 2.5 and 400 µM, doing this separately for each of the two antibiotics and for both barks. For all antibiotics, 0.01 M NaCl was used as the ionic background electrolyte. The use of different concentrations, as well as different bio-adsorbent:solution ratios, was due to the lower adsorption of Cla compared to the other two antibiotics, observed in previous studies [33]. The suspensions of bio-adsorbent with antibiotic were shaken for 48 h at 50 rpm on a rotary shaker, in the dark, and at room temperature (25 ± 1 °C). A time of 48 h of stirring was selected after having carried out studies of the adsorption kinetics and determining that equilibrium was reached after that stirring period.

After 48 h of agitation, the samples were centrifuged at 4000 rpm for 15 min in a Rotina 35 R centrifuge (Hettich Zentrifugen, Germany), and subsequently filtered through nylon syringe filters (0.45 µm pore size). These filtered samples were transferred to Eppendorf propylene vials to measure the pH using a combined glass micro-electrode (Crison, Spain). The antibiotic concentration was quantified using HPLC equipment, using 2 mL vials.

Besides, the adsorption samples were also analysed by IR with maximum concentration of each antibiotic and by-product (Figs. S3 and S4). This study allows us to know the interactions between antibiotics and the surface of the by-products. The spectra were obtained by transmittance using KBr pellets and the same conditions previously reported for by-products.

In the case of the desorption process, the samples previously used to study adsorption were weighed to determine the weight of the bio-adsorbent and also the amount of solution with antibiotic that was

occluded in that sorbent material, and then the bio-adsorbent was resuspended in 20 or 40 mL (depending on the antibiotic) of 0.01 M NaCl. These samples were shaken for 48 h and then centrifuged, filtered and the antibiotic concentrations were quantified in the same way as in the samples from the adsorption studies.

In the case of the samples used for the adsorption-desorption studies as a function of pH, the experiment was carried out at pH between 3 and 10, adjusting with different volumes of 0.5 M HCl and 0.5 M NaOH. In the case of Cla, the concentration of antibiotic added was 100 μM , with a bioadsorbent:solution ratio of 0.5:20. For Tri and Cip, an initial concentration of 400 μM and a ratio of 0.5:40 was used. The differences in the bioadsorbent:solution ratio and in the concentration among antibiotics are for the same reason explained previously. As in the previous experiment, the background electrolyte was 0.01 M NaCl. The suspensions were shaken at 50 rpm for 48 h, in the dark, and centrifuged at 4000 rpm for 15 min. Next, the samples were filtered, separating the supernatant with nylon syringe filters, and the solid phase (the bio-adsorbent material) was used for the study of desorption. In the samples, pH was measured using a combined glass micro-electrode, and the antibiotic concentration was determined by means of HPLC. Regarding desorption, the solid samples from the adsorption process were weighed and re-suspended in 20 or 40 mL (depending on the antibiotic) of 0.01 M NaCl, with the addition of HCl or NaOH to maintain the same pH conditions as in the adsorption phase. The samples were shaken, centrifuged, filtered, and measured as in the previous adsorption phase.

2.4. Release experiments

The release experiments were carried out in a stirred flow chamber, consisting of a polypropylene chamber (reactor) with a volume of 1.5 cm^3 and two Teflon filters (0.45 μm pore size), one at the inlet, and another one at the exit, to avoid the loss of bark material.

The reactor inlet is connected to a booster pump (Gilson Minipuls®3), which is responsible for feeding the reactor with the corresponding solution. This pump allows the flow to be determined and constant throughout the experiment. At the outlet, the reactor is connected to a fraction collector (Gilson FC 203 B), which collects the samples leaving the reactor at a fixed time interval. A magnet (3 mm in length and 1 mm in diameter) was placed inside the reactor together with the bark sample, stirring at 400 rpm, guaranteeing homogenization between the bio-adsorbent material and the solution. The experiment is carried out inside a thermostatic chamber that ensures that the temperature remains constant at 25 ± 1 $^\circ\text{C}$ throughout the entire process.

The flow rate is 1.5 mL min^{-1} , and 80 samples of 1.5 mL each were collected, so the collection time for each of them was 1 min, thus obtaining a total collection time of 80 min.

For the release of the three antibiotics from both barks, solutions of 0.01 M NaCl were used, adjusting the pH to values of 3.0, 5.0 and 8.0 with solutions of 0.5 M HCl and 0.5 M NaOH. Regarding the preparation of the sample, 0.2 g of pine bark was taken, being the weight of 0.025 g in the case of cork oak bark (due to its density, since the same amount as that used for pine bark would occupy the entire reactor and the homogeneity of the sample would not be guaranteed). Once weighed, 200 μL of acetone were added to eliminate any microorganism present in the bark materials and avoid the possibility of biodegradation of the antibiotics. Once these bark samples were dry, 100 μL of the antibiotic solution were added, obtaining a final concentration of 250 mg kg^{-1} . Since the amount of bark varies depending on whether it is pine or cork oak, the initial concentration of antibiotic added also varies, but always obtaining the same final concentration mentioned. The material is left in the dark for 24 h to facilitate the evaporation of the sample and avoid photo-degradation. After 24 h, the magnet is inserted and, once the reactor is closed, the 0.01 M NaCl solution is passed through at the corresponding pH value. During the 80 min that the experiment lasts, the samples are collected, the pH is measured in each of them, and they are transferred to 2 mL vials to later measure the antibiotic

concentration by HPLC.

2.5. Quantification of the antibiotics

The antibiotic quantification methodology has been detailed in previous studies [34]. Briefly, the quantification of each of the antibiotics is carried out in an HPLC unit (Ultimate 3000 HPLC, Thermo Fisher Scientific, Madrid, Spain). Chromatographic separations were carried out on a C18 analytical column supplied by Phenomenex (Madrid, Spain). The injection volume is 50 μL for Cip and Tri, and 200 μL for Cla, and the established flows are 1.5 mL min^{-1} and 1.0 mL min^{-1} , respectively. The mobile phases used were acetonitrile and 0.01 M phosphoric acid for Cip and Tri, and acetonitrile and 0.025 M monopotassium phosphate for Cla. For Tri and Cip, the analysis time was 15 min, with retention times being 5.6 and 6.5 min, respectively. In the case of Cla, the total time was 25 min, and the retention time was 13.6 min. The wavelengths used were 210 nm for Tri and Cip, and 212 nm for Cla.

2.6. Statistical analyses and data treatment

The data obtained from the equilibrium adsorption experiments were described using the Freundlich (Eq. 1) and Linear (Eq. 2) models widely used by other authors [10,35]:

$$q_a = K_F C_{eq}^n \quad (1)$$

$$q_a = K_d C_{eq} \quad (2)$$

where q_a ($\mu\text{mol kg}^{-1}$) is the amount of each antibiotic adsorbed at equilibrium; C_{eq} ($\mu\text{mol L}^{-1}$) is the concentration of each antibiotic that remains in the equilibrium solution; K_F ($\text{L}^n \mu\text{mol}^{1-n} \text{kg}^{-1}$) is the Freundlich affinity coefficient; n (dimensionless) is the Freundlich linearity index; K_d (L kg^{-1}) is the distribution constant in the Linear model.

The model used to calculate the adsorption coefficients (K_d) corresponds to the different forms of the antibiotics (K_d^+ is the adsorption coefficient for the positively charged form of the antibiotic; K_d^0 is the coefficient for the zwitterion form; K_d^- is the coefficient for the negatively charged form) [36]. Eq. (3) (Eq. 3) was used to calculate them:

$$K_d = (K_d^+ \alpha^+) + (K_d^0 \alpha^0) + (K_d^- \alpha^-) \quad (3)$$

In this equation, K_d is the total adsorption coefficient (L kg^{-1}), which is calculated at different pHs. α is the fraction of each antibiotic species as a function of pH. Specifically, α^+ , α^0 and α^- represent the proportion of the different chemical species of the antibiotic obtained from the dissociation constants (pK_a values) [37,38]. K_d^+ is the adsorption coefficient for the positively charged form of the antibiotic; K_d^0 is the coefficient for the zwitterion form, and K_d^- is the coefficient for the negatively charged form.

The accumulated amount of antibiotics obtained from the release experiments was calculated using Eq. (4) (Eq. 4) used by Cutillas-Barreiro et al. [14]:

$$q(i) = \left\{ \sum_{j=1}^i \left[\frac{(C_1(i) - C_2(i)) \Delta t}{V_e} J_w \right] + [C_1(i+1) - C_2(i+1)] \right\} \frac{V_e}{m} \quad (4)$$

Where $q(i)$ is the concentration of antibiotic released ($\mu\text{mol kg}^{-1}$); Δt is the time interval at which each sample is collected (minutes); $C_1(i)$ and $C_2(i)$ are the concentrations of antibiotic in each sample at the reactor outlet in the presence and absence of bark ($\mu\text{mol L}^{-1}$); $C_1(i+1)$ and $C_2(i+1)$ are the concentrations of antibiotic in the stirred flow chamber in the presence and absence of bark ($\mu\text{mol L}^{-1}$); J_w is the flow rate (mL min^{-1}); V_e is the effective volume of solution in the reactor chamber (mL); m is the sample of bark (g).

The data obtained from the release experiments were adjusted to

pseudo-first-order (Eq. 5) and pseudo-second-order (Eq. 6) models, being the expressions, respectively:

$$q_a = q_e(1 - e^{-k_1 t}) \quad (5)$$

$$q_a = \frac{k_2 q_e^2 t}{1 + k_2 q_e t} \quad (6)$$

where q_a ($\mu\text{mol kg}^{-1}$) is the total amount of antibiotic released at a moment t (min); q_e ($\mu\text{mol kg}^{-1}$) is the amount of antibiotic released at equilibrium; k_1 (min^{-1}) and k_2 ($\text{kg } \mu\text{mol}^{-1} \text{ h}^{-1}$) are the pseudo-first-order and pseudo-second-order kinetic constants, respectively [39]. The SPSS software (version 21) was used to perform the adjustments of the experimental data to the different models.

3. Results and discussion

3.1. Characteristics of the bio-adsorbents

The characteristics of both bio-adsorbents: pine bark (PB) and cork oak bark (OB) are listed in Table S1. They present very different characteristics; specifically, in the case of organic carbon content, the cork oak bark has a higher content (60.4%) compared to pine bark (48.7%), as it occurs with the phosphorus content (165.5 mg kg^{-1} in the case of OB and 70.5 mg kg^{-1} for PB), or the surface area (0.89 $\text{m}^2 \text{g}^{-1}$ for OB, and 0.36 $\text{m}^2 \text{g}^{-1}$ for PB). However, pine bark presents higher values for the nitrogen content (13.2%) and the effective cation exchange capacity ($e\text{CEC}$) (14.9 $\text{cmol}_c \text{kg}^{-1}$ with respect to the cork oak bark (with values of 0.6% N, and 11 $\text{cmol}_c \text{kg}^{-1}$ for $e\text{CEC}$, respectively). Also, both bio-adsorbents were characterised before the adsorption by FTIR, evidencing typical characteristics for both compounds explained in Supplementary Material (Figs. S1 and S2).

3.2. Adsorption/desorption experiments

Fig. 1 shows the adsorption curves for the three antibiotics (Cip, Cla and Tri), and for both bark materials: pine (PB), on the left, and cork oak (OB), on the right. They represent the amount adsorbed (q_a in $\mu\text{mol kg}^{-1}$) and the concentration present at equilibrium (C_e in $\mu\text{mol L}^{-1}$).

Among the three antibiotics, Cip is the one with the highest adsorption capacity, with greater adsorption as the initial concentration increases, which is reflected in the adsorption curves, as well as in Tables S3 and S4, where the amount of antibiotic adsorbed for each initial concentration is indicated, as well as the corresponding adsorption percentage. For the same initial concentration of 100 $\mu\text{mol L}^{-1}$, the amount of Cip adsorbed is 8075.2 $\mu\text{mol kg}^{-1}$ in the case of pine bark,

Table 1

Values of the adsorption capacity or removal efficiency of Ciprofloxacin, Clarithromycin and Trimethoprim by different by-products.

| Antibiotic | Adsorbent | Adsorption capacity /Removal efficiency | Reference |
|----------------|---|---|-----------|
| Ciprofloxacin | Straw (Biochar) | 93.3% | [42] |
| | Sesame Straw (Biochar) | 185.7 mg g^{-1} | |
| Clarithromycin | Rice Straw (Biochar) | 747.6 mg g^{-1} | |
| | Activated carbon | 246.7 mg g^{-1} | [43] |
| | Activated carbon fibre | 191.7 mg g^{-1} | |
| | Bentonite clay | 305.2 mg g^{-1} | |
| | Tea-leaf (Biochar) | 238 mg g^{-1} | [44] |
| Trimethoprim | Activated carbon fibre | 70.9 mg g^{-1} | [43] |
| | Cuttlefish bone powder | 34.5 mg g^{-1} | [45] |
| Trimethoprim | Corn Straw Biochar) | 584.2 mg g^{-1} | [42] |
| | Activate carbon | 135 mg g^{-1} | |
| | Magnetite nanoparticles (Fe_3O_4) | > 90% | [46] |

while it is 7371.4 $\mu\text{mol kg}^{-1}$ for cork oak bark. This difference between both barks may be due to the variability in the $e\text{CEC}$. Figueroa-Diva et al. [40], have seen that the adsorption of fluoroquinolones is strongly influenced by this characteristic. In this case, both barks have different $e\text{CEC}$ values, which can be associated with a higher Cip adsorption for PB than for OB (as shown in Table S1), since PB has higher $e\text{CEC}$ than OB.

Fig. 1 also shows that the adsorption curves lack linearity for the three antibiotics, but in the case of Tri and Cla, they present a greater curvature than for Cip. Its behaviour is different since as the initial concentration increases, the adsorption does not increase, with the highest adsorption percentages corresponding to the lowest initial concentrations. This is also reflected in the parameters obtained from the adjustments of the experimental data to the Freundlich and Linear adsorption models.

In the case of Tri, the adsorbed concentration for an initial concentration of 100 $\mu\text{mol L}^{-1}$ corresponds to 7681.5 $\mu\text{mol kg}^{-1}$ for pine bark, and 6696.0 $\mu\text{mol kg}^{-1}$ for cork oak bark, being (as with Cip), higher for PB than for OB. Regarding Cla, the amount adsorbed for the same initial concentration (100 $\mu\text{mol L}^{-1}$) is lower than that of the other antibiotics, being 3684.8 $\mu\text{mol kg}^{-1}$ in the case of pine bark, while the values are slightly lower in the case of cork oak bark (2590.7 $\mu\text{mol kg}^{-1}$). This is in accordance with results obtained by other authors in Table 1, which shows the adsorption capacity or removal efficiency for three antibiotics objects of study. Rath et al. [41] also obtained that macrolides are

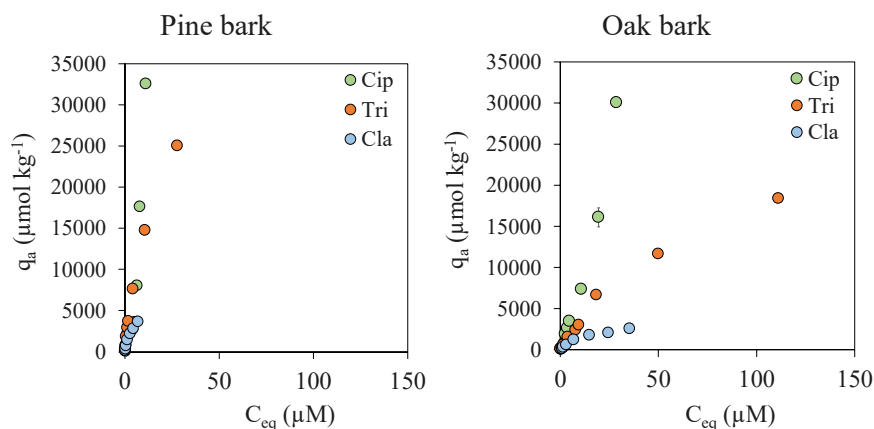


Fig. 1. Adsorption curves of the three antibiotics (Cip, Tri and Cla) on both bio-adsorbents used, pine bark, and oak bark. C_{eq} : antibiotic concentration in the equilibrium solution, q_a : the amount of antibiotic adsorbed on each of both bio-adsorbents. Error bars represent twice the standard deviation of the mean ($n = 3$). When the bars are not visible, it means that they are smaller than the symbols.

Table 2

Parameters resulting from the adjustment of the experimental adsorption data to the Freundlich and Linear models.

| | | Freundlich | | | Linear | |
|-----|----|----------------|-------------|-------|----------------|-------|
| | | K_F | n | R^2 | K_d | R^2 |
| Cip | PB | 126.6 ± 59.3 | 2.31 ± 0.20 | 0.981 | 2172.3 ± 296.5 | 0.800 |
| | OB | 283.9 ± 68.4 | 1.38 ± 0.07 | 0.994 | 938.6 ± 49.6 | 0.966 |
| Cla | PB | 1187.8 ± 61.2 | 0.59 ± 0.03 | 0.994 | 607.1 ± 54.2 | 0.872 |
| | OB | 371.3 ± 65.0 | 0.55 ± 0.06 | 0.975 | 84.9 ± 9.4 | 0.783 |
| Tri | PB | 2979.1 ± 208.4 | 0.65 ± 0.02 | 0.996 | 991.1 ± 79.1 | 0.920 |
| | OB | 806.9 ± 128.8 | 0.67 ± 0.04 | 0.991 | 183.1 ± 14.3 | 0.920 |

PB: Pine bark, OB: Oak bark. K_F ($L^n \mu\text{mol}^{1-n} \text{kg}^{-1}$) is the Freundlich affinity coefficient; n (dimensionless) is the Freundlich linearity index; K_d ($L \text{kg}^{-1}$): is the distribution constant in the Linear model; R^2 : is the coefficient of determination. (Data showed as average values ± standard error).

Table 3Amount of ciprofloxacin (Cip) and trimethoprim (Tri) desorbed at equilibrium ($\mu\text{mol kg}^{-1}$) and percentage desorption (in brackets) for each of the initial concentrations (C_0) used, and for both bio-adsorbents.

| C_0 ($\mu\text{mol L}^{-1}$) | Cip | | Tri | | C_0 ($\mu\text{mol L}^{-1}$) | Cla | |
|----------------------------------|-------------|-------------|--------------|---------------|----------------------------------|--------------|-------------|
| | Pine bark | Oak bark | Pine bark | Oak bark | | Pine bark | Oak bark |
| 2.5 | 5.7 (7.0) | 1.9 (2.8) | 0.5 (0.3) | 27.8 (14.8) | 5 | 50.2 (28.7) | 2.7 (1.7) |
| 5 | 6.6 (1.5) | 2.3 (2.3) | 3.5 (1.0) | 32.8 (10.5) | 10 | 64.9 (18.0) | 8.4 (2.6) |
| 10 | 3.7 (0.4) | 6.0 (0.8) | 10.5 (1.4) | 61.3 (9.6) | 20 | 90.6 (12.2) | 25.2 (3.8) |
| 25 | 8.6 (0.4) | 10.7 (0.6) | 35.1 (1.9) | 151.2 (9.5) | 40 | 180.9 (12.2) | 37.3 (2.9) |
| 40 | 5.5 (0.2) | 6.9 (0.3) | 62.4 (2.1) | 235.7 (9.6) | 60 | 205.4 (9.2) | 87.0 (4.8) |
| 50 | 17.5 (0.5) | 30.9 (0.9) | 83.5 (2.2) | 304.2 (9.9) | 80 | 376.0 (13.4) | 103.0 (4.9) |
| 100 | 55.2 (0.7) | 117.3 (1.6) | 174.1 (2.3) | 636.8 (9.5) | 100 | 568.3 (15.4) | 184.9 (7.1) |
| 200 | 120.5 (0.7) | 311.1 (1.9) | 456.9 (3.1) | 1396.2 (12.0) | | | |
| 400 | 148.8 (0.5) | 699.5 (2.3) | 1263.3 (5.0) | 3423.6 (18.6) | | | |

generally less adsorbed than other families of antibiotics, such as fluoroquinolones.

Therefore, considering both bio-adsorbents, the adsorption values are higher in pine bark for all antibiotics, which may be related to the difference in the surface area (BET) of the two by-products, but despite the differences, both are able to adsorb antibiotics. These results may be due to the amphoteric nature of the three antibiotics, since at pH 4.0 (pH of both barks), the three antibiotics are in their cationic form, and the deprotonated carboxyl groups of the barks make that electrostatic interactions between these bio-adsorbents and antibiotics are established, which was also previously found for other antibiotics, such as sulfonamides [35]. To complete adsorption results, the IR analysis shows the implication of the functional groups mentioned above and the bio-adsorbents present. The FTIR spectra before and after the adsorption of the antibiotics in each bio-adsorbent are explained in Supplementary Material (Figs. S3 and S4).

Table 2 shows the parameters resulting from the adjustment to the adsorption models. Judging by the R^2 values (which vary between 0.975 and 0.996 for Freundlich and between 0.800 and 0.966 for the Linear model), both describe satisfactorily the experimental data. Regarding the Freundlich affinity coefficient, K_F , trimethoprim is the antibiotic that presents the highest values (806.9 and 2979.1 $L^n \mu\text{mol}^{1-n} \text{kg}^{-1}$, for PB and OB, respectively) in both bio-adsorbents. The values are higher for pine bark (126.6 – 2979.1 $L^n \mu\text{mol}^{1-n} \text{kg}^{-1}$) than for cork oak (126.6 – 806.9 $L^n \mu\text{mol}^{1-n} \text{kg}^{-1}$), except in the case of Cip, where it is higher for OB.

Regarding the n parameter, the Freundlich linearity index, the values are below 1 in the case of Cla and Tri (between 0.55 and 0.67), which also indicates that the degree of adsorption decreases as the initial concentration increases, as mentioned above. In the case of ciprofloxacin, the values of n are above 1, indicating that the higher the initial concentration, the greater the adsorption.

Regarding the Linear model, the values of the distribution constant, K_d , vary between 84.9 and 2172.3 $L \text{kg}^{-1}$, with the antibiotic ciprofloxacin presenting the highest value in both bio-adsorbents (938.6 and 2172.3 $L \text{kg}^{-1}$ for PB and OB, respectively), coinciding with what was previously observed by authors such as Figueroa-Diva et al. [40], who obtained that, among different antibiotics, Cip is one with the highest

values for the coefficient of adsorption (K_d). The strong adsorption of Cip in soils [29,41], or in sewage sludge, has been widely studied [47]. In the current research, regarding the K_d values, the sequence from higher to lower concentration is Cip > Tri > Cla, for both bio-adsorbents.

On the other hand, regarding desorption, in Fig. S5 the curves represent the amount of each antibiotic retained (q_d) versus the amount in the equilibrium solution (C_{eq}). In the case of Cip, the curves indicate a lower amount of antibiotic in the equilibrium solution, since both lines are closer to the axis and, therefore, after a desorption cycle, an important part of Cip is retained in the bio-adsorbents. In the case of the other two antibiotics, Cla and Tri, the same happens after a desorption cycle, as a considerable part of the antibiotic is retained in the bio-adsorbents. In the case of Tri, it is shown that there is a greater slope of the desorption curves with respect to the adsorption curves, which indicates the presence of some hysteresis in the desorption process [48]. Table 3 shows the amount desorbed at equilibrium (in $\mu\text{mol kg}^{-1}$ and the desorption percentage in parentheses), indicating that the desorption percentages vary between 0.2% and 7% in the case of Cip, between 0.3% and 18.6% for Tri, and between 1.7% and 28.7% for Cla, evidencing that this last antibiotic presents greater desorption, specifically in the case of pine bark.

Table 4 shows the parameters corresponding to the adjustments of the desorption experimental data to the Freundlich and Linear models. Both models satisfactorily fit the experimental data, since the R^2 values are greater than 0.928 for Freundlich and greater than 0.776 for the Linear model.

Regarding the Freundlich affinity coefficient for desorption, $K_{F(des)}$, it varies between 389.7 and 12016.4 $L^n \mu\text{mol}^{1-n} \text{kg}^{-1}$, the highest values corresponding to pine bark, specifically being between 389.7 and 12016.4 $L^n \mu\text{mol}^{1-n} \text{kg}^{-1}$, while for OB they are between 1069.4 and 5929.7 $L^n \mu\text{mol}^{1-n} \text{kg}^{-1}$. Among the antibiotics, Cip presents the highest values (12016.4 and 5929.7 $L^n \mu\text{mol}^{1-n} \text{kg}^{-1}$), and therefore it is the antibiotic with the lowest desorption. In the case of Cip, as for Tri, the highest values of $K_{F(des)}$ correspond to pine bark.

The values of the linearity coefficient, n , vary between 1.42 and 0.57, with the exception of Cip in pine bark. When these values are less than 1, they indicate the heterogeneity of the adsorption sites. Regarding the distribution coefficient, K_d , the highest values also correspond to Cip

Table 4

Parameters resulting from the adjustment of the experimental desorption data to the Freundlich and Linear models.

| | | Freundlich | | | Linear | |
|-----|----|------------------|---------------|-------|-----------------|-------|
| | | K_F (des) | n (des) | R^2 | K_d (des) | R^2 |
| Cip | PB | 12016.4 ± 1747.6 | 1.42 ± 0.25 | 0.965 | 14757.6 ± 941.2 | 0.951 |
| | OB | 5929.7 ± 401.7 | 0.71 ± 0.03 | 0.995 | 3311.4 ± 178.3 | 0.965 |
| Cla | PB | 389.7 ± 118.4 | 0.80 ± 0.13 | 0.928 | 245.8 ± 19.7 | 0.896 |
| | OB | 1069.4 ± 83.8 | 0.57 ± 0.07 | 0.969 | 633.5 ± 70.4 | 0.776 |
| Tri | PB | 4238.9 ± 352.7 | 0.63 ± 0.03 | 0.991 | 1649.8 ± 148.5 | 0.899 |
| | OB | 1371.3 ± 248.9 | 0.65 ± 0.05 | 0.976 | 396.0 ± 38.4 | 0.876 |

K_F (des) ($L^n \mu mol^{1-n} kg^{-1}$) is the Freundlich affinity coefficient; n (des) (dimensionless) is the Freundlich linearity index; K_d (des) ($L kg^{-1}$): distribution constant in the Linear model; R^2 : coefficient of determination. (Data showed as average values ± standard error).

(14757.6 and 3311.4 $L kg^{-1}$), as in adsorption, and, again as in adsorption, the values are higher for pine bark than for cork oak.

3.2.1. Influence of pH on the adsorption-desorption processes

Batch type experiments were carried out to study the adsorption-desorption process as a function of pH in both bio-adsorbents. Fig. 2 shows the adsorption results for the three antibiotics in both barks. Cip concentration presents a maximum in a pH range between 5 and 7 and then decreases as the pH increases, a behaviour previously observed in soils by other authors [41,49]. The decrease in adsorption at basic pH may be due to the amphoteric nature of the antibiotic since at more basic pH it is in its anionic form, which makes it present a certain repulsion due to the negative charges present on the surface of the organic matter that contain both bio-adsorbents [35,50]. This amphoteric character, in turn, favours adsorption at acidic and neutral pH, since the antibiotic is in its cationic form, which promotes electrostatic attractions with the negative charges of the bio-adsorbents [49,51]. Another mechanism of Cip adsorption is hydrogen bonding, which is considered the primary source of adsorption for fluoroquinolones [52]. Cip adsorption is in the range between 82 and 32584 $\mu mol kg^{-1}$ for pine bark, and between 66 and 30048 $\mu mol kg^{-1}$ for cork oak bark.

In the case of the antibiotic Cla, adsorption is less than 4433.4 $\mu mol kg^{-1}$ for cork oak bark and less than 2964.5 $\mu mol kg^{-1}$ for pine bark. The adsorption as a function of the pH is relatively constant (without presenting many variations with the increase or decrease of the pH), which may be due to the fact that the pK_a presented by the antibiotic is above 9. Below this value, Cla is found in its cationic form, through protonation of the basic dimethylamino group, which causes it to bind to the surface of negatively charged bio-adsorbents [53]. The way to bind is mainly through cationic exchange, although electrostatic interactions can be established between the negative charges of the barks and the antibiotic [54].

The adsorption range of Tri is between that of the Cip and Cla values, specifically between 183 and 25059 $\mu mol kg^{-1}$ for pine bark, and between 187 and 18445 $\mu mol kg^{-1}$ for cork oak bark. For this antibiotic, the adsorption curves for both bio-adsorbents present a maximum at around pH 6.0, similar to that obtained by Franklin et al. [48] who

associate this maximum adsorption with a strong interaction between the antibiotic in its predominantly cationic form and cation exchange sites of the adsorbents. At more acidic or basic pH values, the antibiotic concentration decreases. From the most acidic pHs to the maximum adsorption (which is reached at around neutral pHs), Tri is found in its cationic and neutral forms, so the adsorption mechanisms can be a cationic exchange, hydrogen bonding, and Van der Waals forces [55].

The three antibiotics present two pK_a values (Table S2), which implies that they will have three species depending on the pH, and this characteristic means that the adsorption mechanisms are different for each one of them, as mentioned above and as shown in Fig. 3, where the mechanisms for each antibiotic are listed.

The species for Cip are Cip^+ in acidic conditions, Cip^0 at neutral pH values, and Cip^- at basic pHs. In the case of Cla, $Cl a^+$ from acidic conditions up to pH 9, $Cl a^0$ in the range of 9–12.5, and $Cl a^-$ in very basic conditions. For this antibiotic, the K_d values were not calculated since the experimental data did not fit the equation (Eq. 3). Finally, for trimethoprim, Tri^+ is present at acidic pHs, Tri^0 in the range between 6 and 7, and Tri^- in basic conditions. The K_d values of the different species were calculated using the equation (Eq. 3), and the results obtained are included in Table 5. In fact, Table 5 collects the values of each of the coefficients as a function of speciation, for the two bio-adsorbents and for the Cip and Tri antibiotics. The highest values correspond to ciprofloxacin for the cationic species, which varies between 12.7 and 58.0 $L kg^{-1}$ for both bio-adsorbents, while for trimethoprim, the highest values correspond to the zwitterionic species, with a range between 5.8 and 48.2 $L kg^{-1}$ also for both bio-adsorbents, which corresponds to the maximum adsorption observed in Fig. 2.

Regarding desorption, Fig. 4 shows that the highest desorption percentage (63.6%) corresponds to the antibiotic Cla. This percentage is desorbed from pine bark, and this maximum corresponds to a pH of around 7.0. For the same antibiotic, but in the case of the other bio-adsorbent (OB), the desorption is minimal, being between 0.3% and 3.1%.

In the case of the antibiotic Tri, the maximum desorption is similar for both barks, with values of 48.4% and 47.3%, for OB and PB, respectively, coinciding in both cases with basic pH, above 10. Franklin

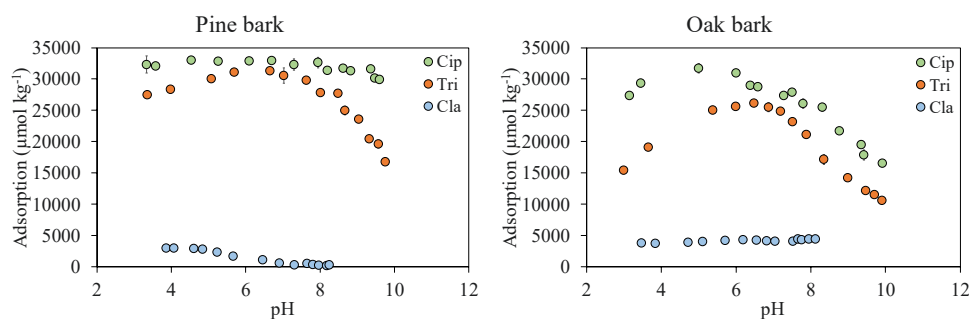


Fig. 2. Adsorption of the three antibiotics (Cip, Tri and Cla) on both bio-adsorbents used, pine bark and oak bark, as a function of pH. Error bars represent twice the standard deviation of the mean ($n = 3$). When the bars are not visible, it means that they are smaller than the symbols.

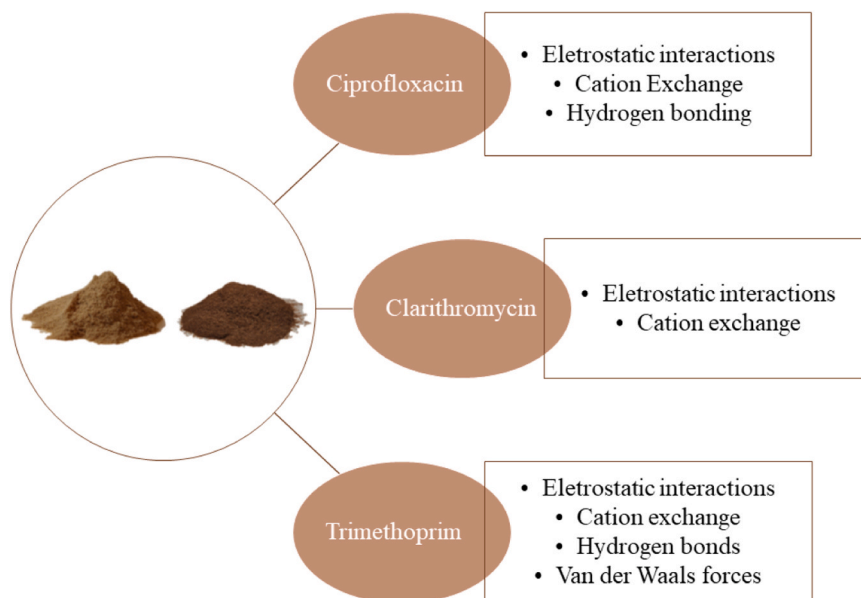


Fig. 3. Adsorption mechanisms of Ciprofloxacin, Clarithromycin and Trimethoprim.

Table 5

K_d values ($L \text{ kg}^{-1}$) for the different forms of ciprofloxacin and trimethoprim.

| | $K_d\text{CIP}^+$ | $K_d\text{CIP}^0$ | $K_d\text{CIP}^-$ | R^2 |
|----|-------------------|-------------------|-------------------|-------|
| PB | 58.0 ± 8.7 | 34.3 ± 9.7 | nd | 0.614 |
| OB | 12.7 ± 3.2 | 3.7 ± 2.9 | nd | 0.416 |
| | $K_d\text{TRI}^+$ | $K_d\text{TRI}^0$ | $K_d\text{TRI}^-$ | R^2 |
| PB | 9.0 ± 1.5 | 48.2 ± 3.3 | 1.4 ± 1.1 | 0.938 |
| OB | 1.5 ± 0.3 | 5.8 ± 0.5 | 0.5 ± 0.2 | 0.887 |

K_d^+ ($L \text{ kg}^{-1}$): adsorption coefficient for the positively charged form; K_d^0 ($L \text{ kg}^{-1}$): adsorption coefficient for the zwitterionic form; K_d^- ($L \text{ kg}^{-1}$): adsorption coefficient for the negatively charged form. The coefficients have been calculated using Eq. (3). R^2 : coefficient of determination.

et al. [48] pointed out that at basic pH the antibiotic is in its negative form, which is why it presents fewer interactions with the negative charges of the bio-adsorbents, and hence the greater desorption.

In the case of Cip, the maximum percentage of desorption is (as in Tri) above 10, presenting maximum values of 32.6% and 32.7% for PB and OB, respectively. This low desorption of Cip may be associated with its low water solubility [2].

3.3. Release experiments

In addition to the batch experiments, the release of the three antibiotics from both barks was studied at three different pHs. It was carried

Table 6

Mean pH values of the samples for each antibiotic, varying the pH of the solution used for release (data showed as average values \pm standard deviation).

| | pH 3.0 | pH 5.0 | pH 8.0 |
|-----|---------------|---------------|---------------|
| Cip | | | |
| PB | 3.4 ± 0.1 | 3.9 ± 0.3 | 4.3 ± 0.3 |
| OB | 3.0 ± 0.2 | 5.1 ± 0.3 | 6.1 ± 0.9 |
| Cl | | | |
| PB | 3.3 ± 0.2 | 4.5 ± 0.2 | 4.9 ± 0.5 |
| OB | 2.4 ± 0.1 | 4.9 ± 0.4 | 6.5 ± 0.7 |
| Tri | | | |
| PB | 3.1 ± 0.1 | 4.2 ± 0.3 | 4.9 ± 0.6 |
| OB | 3.1 ± 0.0 | 5.0 ± 0.6 | 6.4 ± 0.2 |

out by means of stirred flow chamber release experiments, performed at three different pH values (3.0, 5.0 and 8.0). Despite the fact that the initial solutions had these three pH values, the pH at which each of the experiments took place was different depending on the bio-adsorbent. Table 6 indicates that in the case of pH 3.0, it was maintained throughout the experiment, but in the case of pH 5.0 and 8.0, pine bark was capable of buffering the pH of the solution, obtaining a pH of around 4.0 instead of 5.0, and close to 5.0 in the case of the pH 8.0 solution. Cork bark was also capable of buffering, maintaining the pH of the release process at pH 8.0 at a real value of around 6.0.

Fig. 5 shows the release of the three antibiotics as a function of the three pH values, for pine bark. As observed in the figure, the change in pH only causes significant modifications in the release of Cla. For Cip

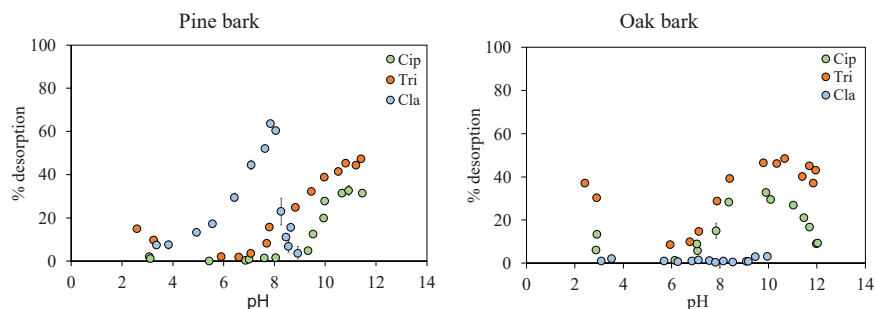


Fig. 4. Desorption percentages for the three antibiotics (Cip, Tri and Cla) as a function of pH, for both bio-adsorbents used, pine bark and oak bark. Error bars represent twice the standard deviation of the mean ($n = 3$). When the bars are not visible, it means that they are smaller than the symbols.

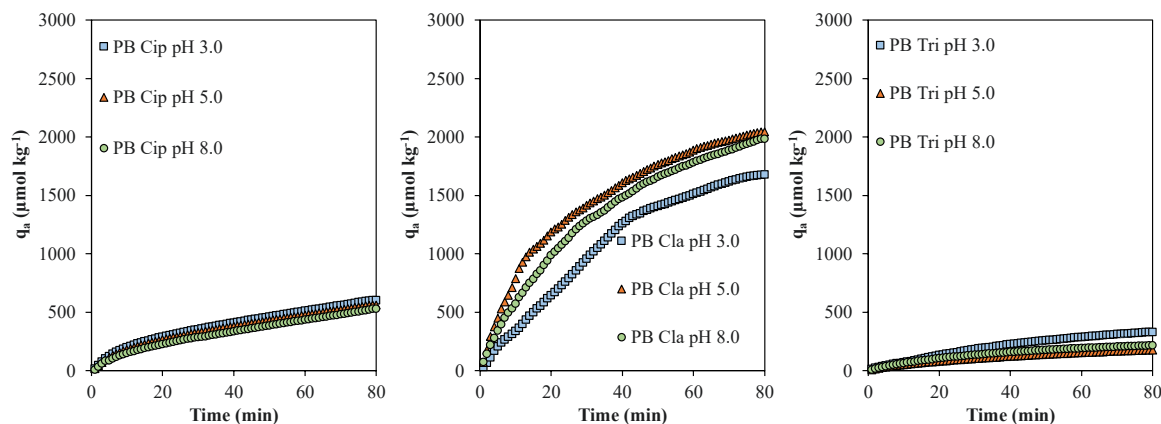


Fig. 5. Release of Cip, Cla, and Tri from pine bark (PB) at the three studied pHs: 3.0, 5.0 and 8.0. q_a : cumulative amount of Cip, Cla or Tri released at the three pHs.

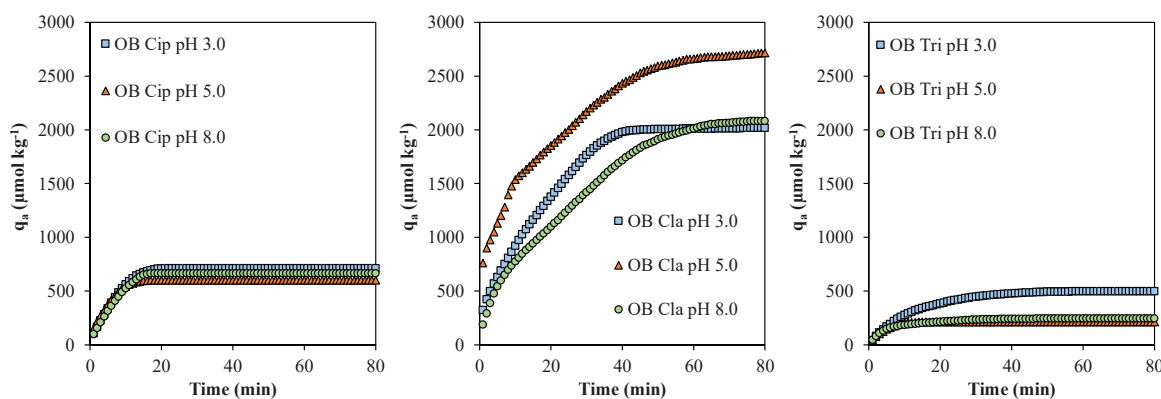


Fig. 6. Release of Cip, Cla, and Tri from oak bark (OB) at the three studied pHs: 3.0, 5.0 and 8.0. q_a : cumulative amount of Cip, Cla or Tri released at the three pHs.

and Tri, the release of both antibiotics does not exceed 600.3 and 330.2 $\mu\text{mol L}^{-1}$, respectively, and these values are similar for the three pH values.

On the other hand, in the case of Cla, pine bark releases more antibiotic at pH 5.0 and 8.0 than at pH 3.0, reaching a maximum of 2044.7 $\mu\text{mol L}^{-1}$ at pH 5.0.

In the case of cork oak bark, Fig. 6 shows that the release is higher than in the case of pine bark, for the three antibiotics. The figure shows that Cla continues to be the most mobile antibiotic, presenting higher amounts of antibiotic released, reaching a maximum of 2715.1 $\mu\text{mol L}^{-1}$ at pH 5.0. In the case of this bark (OB), regarding Tri a small difference can be observed at pH 3.0, whose release (499.4 $\mu\text{mol L}^{-1}$) is greater than that at the other two pHs. This greater release at acidic pH can be associated with the fact that, under these pH conditions, the antibiotic is in its cationic form, which can generate a certain electrostatic repulsion with the positive surface in both bio-adsorbents, since in PB it is also present. A small difference can be distinguished between pH 3.0 and the other pHs, with pH 3 being the one with the highest release. At pH 3.0, the amount of H^+ on the surface of the bio-adsorbents is higher, hence more release takes place than at high pHs [56]. And in the case of Cip, as for pine bark, the release is not influenced by the pH, presenting the maximum value of 710.4 $\mu\text{mol L}^{-1}$ at pH 3.0.

A release sequence can be established, going from more to less mobile antibiotics, which would be Cla < Tri < Cip. This indicates that it could be a significant risk of appearance and development of resistance to the antibiotic Cla, which is also reflected in previous studies [57], where the authors indicate that, among the macrolides, Cla is the one presenting a greater risk of developing resistance. The same would occur among the antibiotics that are the subject of this study.

On the other hand, Table 7 shows the values of the parameters

obtained from the adjustments of the experimental data of release of the three antibiotics to the kinetic models of pseudo-first and pseudo-second order that were used in this work. Judging by the R^2 correlation coefficients, both models satisfactorily describe the experimental data, since they present values between 0.923 and 0.999 for the pseudo-first-order model and between 0.927 and 1.000 for the pseudo-second-order model.

Regarding the analysis of the parameters, the kinetic constant (k_1) presents lower values for pine bark (0.018–0.042 min^{-1}) than for cork oak (0.036–0.240 min^{-1}) within each one of the antibiotics, and therefore the release from the cork oak bark is faster. And, comparing the different antibiotics, Tri (0.018 – 0.240 min^{-1}) and Cip (0.021 – 0.217 min^{-1}) present higher values than Cla (0.019 – 0.070 min^{-1}). In the case of Cip, the values are similar to those obtained by other authors as Magesh et al. [58], who find values around 0.029 min^{-1} .

Regarding the amount of antibiotic released at equilibrium (q_e), comparing both bio-adsorbents, for each of the antibiotics, the highest values correspond to cork oak bark (214.6–2646.9 $\mu\text{mol kg}^{-1}$), while the values range between 200.3 and 2212.0 $\mu\text{mol kg}^{-1}$ for pine bark, indicating the best retention of the latter by-product.

Regarding the parameters obtained from the adjustment of the pseudo-second-order model, the kinetic constant (k_2) is higher for cork oak bark (0.000011 – 0.001887 $\text{kg } \mu\text{mol}^{-1} \text{ h}^{-1}$) than for pine bark (0.000004 – 0.000071 $\text{kg } \mu\text{mol}^{-1} \text{ h}^{-1}$). And the antibiotic that presents higher release rates is Tri (0.000019–0.001887 $\text{kg } \mu\text{mol}^{-1} \text{ h}^{-1}$), followed by Cip (0.000018–0.000604 $\text{kg } \mu\text{mol}^{-1} \text{ h}^{-1}$), and finally Cla (0.000004–0.000029 $\text{kg } \mu\text{mol}^{-1} \text{ h}^{-1}$). The amount released at equilibrium, according to the pseudo-second-order model is between 209.1 and 3473.5 $\mu\text{mol kg}^{-1}$ for pine bark, and between 261.2 and 3090.0 $\mu\text{mol kg}^{-1}$ for cork oak bark. Within each of the antibiotics, in

Table 7

Parameters resulting from the adjustment of the experimental release of Cip, Cla and Tri (at different pHs) to pseudo-first and pseudo-second order equations. k_1 (min^{-1}): is the pseudo-first-order kinetics velocity constant; k_2 ($\text{kg } \mu\text{mol}^{-1} \text{h}^{-1}$): is the pseudo-second-order kinetics velocity constant; q_e ($\mu\text{mol kg}^{-1}$): is the amount of antibiotic released at time t at equilibrium; R^2 : coefficient of determination. (Data showed as average values \pm standard error).

| | Pseudo-first order | | | Pseudo-second order | | |
|------------|--------------------|-------------------|-------|-------------------------|--------------------|-------|
| | k_1 | q_e | R^2 | k_2 | q_e | R^2 |
| Cip | | | | | | |
| OB pH 3.0 | 0.151 \pm 0.003 | 716.3 \pm 0.2 | 0.990 | 0.000298 \pm 0.000024 | 782.3 \pm 8.8 | 0.935 |
| OB pH 5.0 | 0.217 \pm 0.003 | 602.1 \pm 1.0 | 0.994 | 0.000604 \pm 0.000043 | 639.8 \pm 4.6 | 0.945 |
| OB pH 8.0 | 0.152 \pm 0.003 | 671.7 \pm 2.3 | 0.985 | 0.000321 \pm 0.000028 | 733.2 \pm 8.2 | 0.927 |
| PB pH 3.0 | 0.028 \pm 0.001 | 633.6 \pm 11.9 | 0.979 | 0.000027 \pm 0.000002 | 877.4 \pm 18.3 | 0.988 |
| PB pH 5.0 | 0.027 \pm 0.001 | 602.3 \pm 11.5 | 0.981 | 0.000026 \pm 0.000002 | 842.9 \pm 17.8 | 0.989 |
| PB pH 8.0 | 0.021 \pm 0.001 | 610.9 \pm 14.5 | 0.985 | 0.000018 \pm 0.000001 | 895.5 \pm 23.8 | 0.990 |
| Cla | | | | | | |
| OB pH 3.0 | 0.060 \pm 0.001 | 2078.9 \pm 13.1 | 0.986 | 0.000026 \pm 0.000002 | 2537.1 \pm 35.8 | 0.974 |
| OB pH 5.0 | 0.070 \pm 0.003 | 2646.9 \pm 30.1 | 0.923 | 0.000029 \pm 0.000002 | 3090.0 \pm 38.7 | 0.963 |
| OB pH 8.0 | 0.036 \pm 0.001 | 2245.6 \pm 23.6 | 0.988 | 0.000011 \pm 0.000001 | 3010.8 \pm 45.8 | 0.989 |
| PB pH 3.0 | 0.019 \pm 0.001 | 2212.0 \pm 44.5 | 0.993 | 0.000004 \pm 0.000000 | 3473.5 \pm 110.6 | 0.991 |
| PB pH 5.0 | 0.042 \pm 0.001 | 2052.8 \pm 16.5 | 0.990 | 0.000015 \pm 0.000000 | 2671.3 \pm 16.9 | 0.998 |
| PB pH 8.0 | 0.030 \pm 0.000 | 2142.8 \pm 9.2 | 0.999 | 0.000008 \pm 0.000000 | 3005.9 \pm 9.1 | 1.000 |
| Tri | | | | | | |
| OB pH 3.0 | 0.077 \pm 0.001 | 500.8 \pm 0.8 | 0.998 | 0.000159 \pm 0.000005 | 589.1 \pm 3.7 | 0.992 |
| OB pH 5.0 | 0.240 \pm 0.003 | 214.6 \pm 0.4 | 0.994 | 0.001887 \pm 0.000148 | 227.2 \pm 1.7 | 0.935 |
| OB pH 8.0 | 0.155 \pm 0.005 | 239.9 \pm 1.1 | 0.966 | 0.000948 \pm 0.000020 | 261.2 \pm 0.7 | 0.995 |
| PB pH 3.0 | 0.018 \pm 0.000 | 429.4 \pm 2.6 | 0.999 | 0.000019 \pm 0.000000 | 668.2 \pm 6.0 | 0.999 |
| PB pH 5.0 | 0.024 \pm 0.001 | 200.3 \pm 2.4 | 0.995 | 0.000065 \pm 0.000002 | 209.1 \pm 3.5 | 0.997 |
| PB pH 8.0 | 0.029 \pm 0.000 | 233.9 \pm 1.4 | 0.998 | 0.000071 \pm 0.000001 | 329.2 \pm 1.1 | 1.000 |

the case of Cla, even though it is released more slowly, it is the most released, presenting values between 2537.1 and 3473.5 $\mu\text{mol kg}^{-1}$. In the case of Cip, the values are slightly lower, being the range between 639.8 and 895.5 $\mu\text{mol kg}^{-1}$, and in the case of Tri, between 209.1 and 668.2 $\mu\text{mol kg}^{-1}$.

Regarding the influence of pH on the release process, for cork oak bark the maximum release rate corresponds to pH 5.0, for the three antibiotics. And in pine bark, for Cla and Tri, the minimum release rate corresponds to pH 3.0.

4. Conclusion

Pine and oak bark are abundant and inexpensive by-products that have demonstrated their ability to adsorb and retain the antibiotics tested in the current study, specifically Cip, Cla and Tri. Pine bark showed the best adsorption results, with Cip and Tri being the most adsorbed. Besides, pine bark showed low desorption values, Cla being the most desorbed antibiotic. Regarding desorption as a function of pH, the three antibiotics showed a similar behaviour: as pH increases, desorption is higher, and reaches a maximum under basic conditions, except for Cla, whose maximum desorption is around neutral pH. From the release experiments, the results also show that Cla is the most mobile antibiotic. In general, applying these forest by-products to retain/remove antibiotics could be a low-cost and effective alternative, helping to face environmental pollution due to the emerging contaminants tested in the study.

CRediT authorship contribution statement

Manuel Arias-Estévez, Esperanza Álvarez-Rodríguez, Paula Pérez-Rodríguez, Avelino Núñez-Delgado, Vanesa Santás-Miguel: Conceptualization. Manuel Arias-Estévez, Esperanza Álvarez-Rodríguez, Andrés Rodríguez-Seijo, Paula Pérez-Rodríguez, Avelino Núñez-Delgado, Vanesa Santás-Miguel: Methodology. Lucía Rodríguez-López, Vanesa Santás-Miguel, Raquel Cela-Dablanca: Software. Manuel Arias-Estévez, Esperanza Álvarez-Rodríguez, Andrés Rodríguez-Seijo, Avelino Núñez-Delgado, Vanesa Santás-Miguel, Raquel Cela-Dablanca: Data curation, Lucía Rodríguez-López, Vanesa Santás-Miguel, Manuel Arias-Estévez, Andrés Rodríguez-Seijo: Writing- Original draft preparation. Manuel Arias-Estévez, Esperanza Álvarez-Rodríguez, Avelino Núñez-Delgado,

Lucía Rodríguez-López, Vanesa Santás-Miguel, Raquel Cela-Dablanca: Visualization. Lucía Rodríguez-López, Vanesa Santás-Miguel, Raquel Cela-Dablanca: Investigation. Manuel Arias-Estévez, Esperanza Álvarez-Rodríguez, Andrés Rodríguez-Seijo, Paula Pérez-Rodríguez, Avelino Núñez-Delgado, Vanesa Santás-Miguel: Supervision. Manuel Arias-Estévez, Esperanza Álvarez-Rodríguez, Andrés Rodríguez-Seijo, Avelino Núñez-Delgado, Vanesa Santás-Miguel: Validation. Avelino Núñez-Delgado, Andrés Rodríguez-Seijo: Writing- Reviewing and Editing.

Declaration of Competing Interest

The authors declare that they have no known competing financial interests or personal relationships that could have appeared to influence the work reported in this paper.

Data Availability

Data will be made available on request.

Acknowledgements

This work was supported by the Spanish Ministry of Science, Innovation and Universities with European Regional Development Funds (FEDER in Spain) [grant numbers RTI2018-099574-B-C21 and RTI2018-099574-B-C22]. The authors would like to recognize the financial support of the "Consellería de Cultura, Educación e Universidade (Xunta de Galicia)" through the contract ED431C2021/46-GCR granted to the research group BV1 of the University of Vigo. LRL holds a pre-doctoral FPU contract (FPU19/03758; Ministry of Universities, Spanish Government), VSM holds a postdoctoral fellowship (ED481B-2022-081; Xunta de Galicia, Spain), PPR and ARS are supported by a JdCi research contract funded by MCIN/AEI/UVigo and European Union EU/PRTR (IJC2020-044426-I/MCIN/AEI/10.13039/501100011033 and IJC2020-044197-I/MCIN/AEI/10.13039/501100011033, respectively). Funding for open access charge: Universidade de Vigo/CISUG.

Appendix A. Supporting information

Supplementary data associated with this article can be found in the online version at [doi:10.1016/j.jece.2023.111437](https://doi.org/10.1016/j.jece.2023.111437).

References

- [1] R. Xiao, D. Huang, L. Du, B. Song, B. Song, L. Yin, Y. Chen, L. Gao, R. Li, H. Huang, G. Zeng, Antibiotic resistance in soil-plant systems: A review of the source, dissemination, influence factors, and potential exposure risks, *Sci. Total Environ.* 869 (2023), 161855, <https://doi.org/10.1016/j.scitotenv.2023.161855>.
- [2] I.T. Carvalho, L. Santos, Antibiotics in the aquatic environments: a review of the European scenario, *Environ. Int.* 94 (2016) 736–757, <https://doi.org/10.1016/j.envint.2016.06.025>.
- [3] F.O. Gudda, M.G. Waigi, E.S. Odinga, B. Yang, L. Carter, Y. Gao, Antibiotic-contaminated wastewater irrigated vegetables pose resistance selection risks to the gut microbiome, *Environ. Pollut.* 264 (2020), 114752, <https://doi.org/10.1016/j.envpol.2020.114752>.
- [4] Q. Zeng, J. Sun, L. Zhu, Occurrence and distribution of antibiotics and resistance genes in greenhouse and open-field agricultural soils in China, *Chemosphere* 224 (2019) 900–909, <https://doi.org/10.1016/j.chemosphere.2019.02.167>.
- [5] S. Li, H. Gao, H. Zhang, G. Wei, Q. Shu, R. Li, S. Jin, G. Na, Y. Shi, The fate of antibiotic resistance genes in the coastal lagoon with multiple functional zones, *J. Environ. Sci.* 128 (2023) 93–106, <https://doi.org/10.1016/j.jes.2022.07.021>.
- [6] C.O. Okoye, R. Nyaruaba, R.E. Ita, S.U. Okon, C.I. Addey, C.C. Ebedo, A. O. Opabunmi, E.S. Okeke, K.I. Chukwudozie, Antibiotic resistance in the aquatic environment: Analytical techniques and interactive impact of emerging contaminants, *Environ. Toxicol. Pharmacol.* 96 (2022), 103995, <https://doi.org/10.1016/j.etap.2022.103995>.
- [7] K.A. Patel, R.R. Singhania, A. Pal, C.-W. Chen, A. Pandey, C.-D. Dong, Advances on tailored biochar for bioremediation of antibiotics, pesticides and polycyclic aromatic hydrocarbon pollutants from aqueous and solid phases, *Sci. Total Environ.* 817 (2022), 153054, <https://doi.org/10.1016/j.scitotenv.2022.153054>.
- [8] M. Stylianou, A. Christou, C. Michael, A. Agapiou, P. Papanastasiou, D. Fatta-Kassinos, Adsorption and removal of seven antibiotic compounds present in water with the use of biochar derived from the pyrolysis of organic waste feedstocks, *J. Environ. Chem. Eng.* 9 (2021), 105868, <https://doi.org/10.1016/j.jece.2021.105868>.
- [9] H.K. An, B.Y. Park, D.S. Kim, Crab shell for the removal of heavy metals from aqueous solution, *Water Resour.* 35 (2001) 3551–3556, [https://doi.org/10.1016/S0043-1354\(01\)00099-9](https://doi.org/10.1016/S0043-1354(01)00099-9).
- [10] R. Cela-Dablanca, A. Barreiro, L. Rodríguez-López, V. Santás-Miguel, M. Arias-Estévez, A. Núñez-Delgado, E. Álvarez-Rodríguez, M.J. Fernández-Sanjurjo, Potential of low-cost bio-adsorbents to retain amoxicillin in contaminated water, *Environ. Res.* 213 (2022), 113621, <https://doi.org/10.1016/j.envres.2022.113621>.
- [11] I. Anastopoulos, I. Pashalidis, A.G. Orfanos, I.D. Manaiotis, T. Tatarchuk, L. Sellaoui, A. Bonilla-Petriciolet, A. Mittal, A. Núñez-Delgado, Removal of caffeine, nicotine and amoxicillin from (waste)waters by various adsorbents. A Review, *J. Environ. Manag.* 261 (2020), 110236, <https://doi.org/10.1016/j.jenvman.2020.110236>.
- [12] R. Han, D. Ding, Y. Xu, W. Zou, Y. Wang, Y. Li, L. Zou, Use of rice husk for the adsorption of congo red from aqueous solution in column mode, *Bioresour. Technol.* 99 (2008) 2938–2946, <https://doi.org/10.1016/j.biortech.2007.06.027>.
- [13] M. Dias, J. Pinto, B. Henriques, P. Figueira, E. Fabre, D. Tavares, C. Vale, E. Pereira, Nutshells as Efficient Biosorbents to Remove Cadmium, Lead, and Mercury from Contaminated Solutions, *Int. J. Environ. Res. Public Health* 18 (2021) 1580, <https://doi.org/10.3390/ijerph18041580>.
- [14] L. Cutillas-Barreiro, L. Ansias-Manso, D. Fernández-Calviño, M. Arias-Estévez, J. C. Nóvoa-Muñoz, M.J. Fernández-Sanjurjo, E. Álvarez-Esperanza, A. Núñez-Delgado, Pine bark as bio-adsorbent for Cd, Cu, Ni, Pb and Zn: Batch-type and stirred flow chamber experiments, *J. Environ. Manag.* 144 (2014) 258–264, <https://doi.org/10.1016/j.jenvman.2014.06.008>.
- [15] D.B. Pal, R. Saini, N. Srivastava, I. Ahmad, M.Y. Alshahrani, V.K. Gupta, Waste biomass based potential bioadsorbent for lead removal from simulated wastewater, *Bioresour. Technol.* 349 (2022), 126843, <https://doi.org/10.1016/j.biortech.2022.126843>.
- [16] J.Z. Lima, A.P. Ogura, L.C.M. da Silva, I.M.R. Nauerth, V.G.S. Rodrigues, E.L. G. Espíndola, J.P. Marques, Biochar-pesticides interactions: An overview and applications of wood feedstock for atrazine contamination, *J. Environ. Chem. Eng.* 10 (2022), 108192, <https://doi.org/10.1016/j.jece.2022.108192>.
- [17] S. Sousa, P. Jiménez-Guerrero, A. Ruiz, N. Ratola, A. Alves, Organochlorine pesticides removal from wastewater by pine bark adsorption after activated sludge treatment, *Environ. Technol.* 32 (2011) 673–683, <https://doi.org/10.1080/09593330.2010.510535>.
- [18] L. Delgado-Moreno, L. Sánchez-Moreno, A. Peña, Assessment of olive cake as soil amendment for the controlled release of triazine herbicides, *Sci. Total Environ.* 378 (2007) 119–123, <https://doi.org/10.1016/j.scitotenv.2007.01.023>.
- [19] M.Á. Olivella, C. Bazzicalupi, A. Bianchi, N. Fiol, I. Villaescusa, New insights into the interactions between cork chemical components and pesticides. The contribution of π - π interactions, hydrogen bonding and hydrophobic effect, *Chemosphere* 119 (2015) 863–870, <https://doi.org/10.1016/j.chemosphere.2014.08.051>.
- [20] Y. Sun, Q. Zhang, J.H. Clark, N.J.D. Graham, D. Hou, Y.S. Ok, D.C.W. Tsang, Tailoring wood waste biochar as a reusable microwave absorbent for pollutant removal: Structure-property-performance relationship and iron-carbon interaction, *Bioresour. Technol.* 362 (2022), 127838, <https://doi.org/10.1016/j.biortech.2022.127838>.
- [21] M.Á. Olivella, I. Fernández, L. Cano, P. Jové, A. Oliveras, Role of chemical components of cork on sorption of aqueous polycyclic aromatic hydrocarbons, *Int. J. Environ. Res.* 7 (2013) 225–234, <https://doi.org/10.22059/ijer.2012.601>.
- [22] FAO, *Food and Agriculture Organization of the United Nations, Forestry Production and Trade*, 2023. (<https://www.fao.org/faostat>) (accessed 2023–05-27).
- [23] E. Vadell, S. de-Miguel, J. Pemán, Large-scale reforestation and afforestation policy in Spain: A historical review of its underlying ecological, socioeconomic and political dynamics, *Land Use Pol.* 55 (2016) 37–48, <https://doi.org/10.1016/j.landusepol.2016.03.017>.
- [24] E. Sánchez-Hernández, V. González-García, J. Casanova-Gascón, J.J. Barrioso-Vargas, J. Balduque-Gil, B. Lorenzo-Vidal, J. Martín-Gil, P. Martín-Ramos, Valorization of *Quercus suber* L. Bark as a Source of Phytochemicals with Antimicrobial Activity against Apple Tree Diseases, *Plants* 11 (2022) 3415, <https://doi.org/10.3390/plants11243415>.
- [25] A.F. Sousa, P.C.R.O. Pinto, A.J.D. Silvestre, C.P. Neto, Triterpenic and Other Lipophilic Components from Industrial Cork Byproducts, *J. Agric. Food Chem.* 54 (2006) 6888–6893, <https://doi.org/10.1021/jf060987>.
- [26] A. Ramos, J. Berzosa, F. Clarens, M.A. Marin, A. Rouboa, Environmental and socioeconomic assessment of cork waste gasification: Life cycle and cost analysis, *J. Clean. Prod.* 249 (2020), 119316, <https://doi.org/10.1016/j.jclepro.2019.119316>.
- [27] A. Sen, H. Pereira, M.A. Olivella, I. Villaescusa, Heavy metals removal in aqueous environments using bark as a biosorbent, *Int. J. Environ. Sci. Technol.* 12 (2015) 391–404, <https://doi.org/10.1007/s13762-014-0525-z>.
- [28] J.O. Ighalo, A.G. Adeniyi, Adsorption of pollutants by plant bark derived adsorbents: An empirical Review, *J. Water Process. Eng.* 35 (2020), 101228, <https://doi.org/10.1016/j.jwpe.2020.101228>.
- [29] L. Rodríguez-López, V. Santás-Miguel, R. Cela-Dablanca, A. Núñez-Delgado, E. Álvarez-Rodríguez, P. Pérez-Rodríguez, M. Arias-Estévez, Ciprofloxacin and Trimethoprim Adsorption/Desorption in Agricultural Soils, *Int. J. Environ. Res. Public Health* 19 (2022) 8426, <https://doi.org/10.3390/ijerph19148426>.
- [30] M.E. Sumner, W.P. Miller, Cation exchange capacity and exchange coefficients, in: D.L. Sparks (Ed.), *Methods of Soil Analysis. Part 3. Chemical Methods, SSSA, Madison, Wisconsin*, 1996, pp. 1201–1229.
- [31] P.M. Bertsch, P.R. Bloom, Aluminium, in: D.L. Sparks (Ed.), *Methods of Soil Analysis Part 3. Chemical Methods. SSSA Book Series: 5, SSSA and ASA, Madison, WI*, 1996, pp. 517–550.
- [32] Olsen, S.R., Sommers, L.E. *Phosphorus*. in: Page, A.L. (Ed.), *Methods of Soil Analysis. Part 2. Chemical and Microbiological Properties. Soil Sci. Soc. Am., Madison*, 1982, pp. 403–430.
- [33] M. Pan, L.M. Chu, Adsorption and degradation of five selected antibiotics in agricultural soil, *Sci. Total Environ.* 545–546 (2016) 48–56, <https://doi.org/10.1016/j.scitotenv.2015.12.040>.
- [34] L. Rodríguez-López, R. Cela-Dablanca, A. Núñez-Delgado, E. Álvarez-Rodríguez, D. Fernández-Calviño, M. Arias-Estévez, Photodegradation of ciprofloxacin, clarithromycin and trimethoprim: Influence of pH and humic acids, *Molecules* 26 (2021) 3080, <https://doi.org/10.3390/molecules26113080>.
- [35] M. Conde-Cid, R. Cela-Dablanca, G. Ferreira-Coelho, D. Fernández-Calviño, A. Núñez-Delgado, M.J. Fernández-Sanjurjo, M. Arias-Estévez, E. Álvarez-Rodríguez, Sulfadiazine, sulfamethazine and sulfachloropyridazine removal using three different porous materials: Pine bark, “oak ash” and mussel shell, *Environ. Res.* 195 (2021), 110814, <https://doi.org/10.1016/j.envres.2021.110814>.
- [36] C. Álvarez-Esmoris, L. Rodríguez-López, A. Núñez-Delgado, E. Álvarez-Rodríguez, D. Fernández-Calviño, M. Arias-Estévez, Influence of pH on the adsorption-desorption of doxycycline, enrofloxacin, and sulfamethoxypyridazine in soils with variable surface charge, *Environ. Res.* 214 (2022), 114071, <https://doi.org/10.1016/j.envres.2022.114071>.
- [37] R. De-Lievie, *Aqueous Acid-Base Equilibria and Titration*, Oxford, New York, USA, 1999.
- [38] C.G. Enke, *The Art and Science of Chemical Analysis*, Wiley, New York, USA, 2001.
- [39] C. Álvarez-Esmoris, M. Conde-Cid, D. Fernández-Calviño, M.J. Fernández-Sanjurjo, A. Núñez-Delgado, E. Álvarez-Rodríguez, M. Arias-Estévez, Adsorption-desorption of doxycycline in agricultural soils: Batch and stirred-flow-chamber experiments, *Environ. Res.* 186 (2020), 109565, <https://doi.org/10.1016/j.envres.2020.109565>.
- [40] R.A. Figueroa-Diva, D. Vasudevan, A.A. MacKay, Trends in soil sorption coefficients within common antimicrobial families, *Chemosphere* 79 (2010) 786–793, <https://doi.org/10.1016/j.chemosphere.2010.03.017>.
- [41] S. Rath, A.H. Fostier, L.A. Pereira, A.C. Dioniso, F.O. Ferreira, K.M. Doretto, L. M. Peruchi, A. Viera, O.F.O. Neto, S.M.D. Bosco, M.J. Martínez-Mija, Sorption behaviors of antimicrobial and antiparasitic veterinary drugs on subtropical soils, *Chemosphere* 214 (2019) 111–122, <https://doi.org/10.1016/j.chemosphere.2018.09.083>.
- [42] X. Zhang, T. Bhattacharya, C. Wang, A. Kumar, P. Veetil Nidheesh, Straw-derived biochar for the removal of antibiotics from water: Adsorption and degradation mechanisms, recent advancements and challenges, *Environ. Res.* 273 (2023), 116998, <https://doi.org/10.1016/j.envres.2023.116998>.
- [43] S. Das, S. Sengupta, Sustainable Removal of Antibiotic Drugs from Wastewater Using Different Adsorbents—a Concise Review, *Water Conserv. Sci. Eng.* 8 (2023) 10, <https://doi.org/10.1007/s41101-023-00180-5>.
- [44] L.M. Madikizela, V.E. Pakade, Trends in removal of pharmaceuticals in contaminated water using waste coffee and tea-based materials with their derivatives, *Water Environ. Res.* 95 (2023), <https://doi.org/10.1002/wer.10857>.
- [45] L. Shearer, S. Pap, S.W. Gibb, Removal of pharmaceuticals from wastewater: A review of adsorptive approaches, modelling and mechanisms for metformin and macrolides, *J. Environ. Chem. Eng.* 10 (2022), 108106, <https://doi.org/10.1016/j.jece.2022.108106>.

- [46] D.M. Nzilu, E.S. Madivoli, Ds Makhano, B.V. Otenda, P.G. Kareru, Pk Kairigo, T. Tuhkanen, Environmental remediation using nanomaterial as adsorbents for emerging micropollutants, *Environ. Nanotechnol. Monit. Manag.* 20 (2023), 100789, <https://doi.org/10.1016/j.enmm.2023.100789>.
- [47] B. Li, T. Zhang, Biodegradation and Adsorption of Antibiotics in the Activated Sludge Process, *Environ. Sci. Technol.* 44 (2010) 3468–3473, <https://doi.org/10.1021/es903490h>.
- [48] A.M. Franklin, C. Williams, D.M. Andrews, J.E. Watson, Sorption and desorption behavior of four antibiotics at concentrations simulating wastewater reuse in agricultural and forested soils, *Chemosphere* 289 (2022), 133038, <https://doi.org/10.1016/j.chemosphere.2021.133038>.
- [49] D. Vasudevan, G.L. Bruland, B.S. Torrance, V.G. Upchurch, A.A. MacKay, pH-dependent ciprofloxacin sorption to soils: Interaction mechanisms and soil factors influencing sorption, *Geoderma* 151 (2009) 68–76, <https://doi.org/10.1016/j.geoderma.2009.03.007>.
- [50] X. Li, T. Liu, X. Han, Y. Li, X. Ma, Removal of heavy metals lead and ciprofloxacin from farm wastewater using peanut shell biochar, *Environ. Technol. Innov.* 30 (2023), 103121, <https://doi.org/10.1016/j.eti.2023.103121>.
- [51] R.M. Pereira-Leal, L.R. Ferracciú-Alleoni, V. Luiz-Torniselo, J. Borges-Regitano, Sorption of fluoroquinolones and sulfonamides in 13 Brazilian soils, *Chemosphere* 92 (2013) 979–985, <https://doi.org/10.1016/j.chemosphere.2013.03.018>.
- [52] V.A. Thai, D.D. Dien, N.T. Thuy, B. Pandit, T.K.Q. Vo, A.P. Khedulkar, Fluoroquinolones: Fate, effects on the environment and selected removal methods, *J. Clean. Prod.* 418 (2023), 137762, <https://doi.org/10.1016/j.jclepro.2023.137762>.
- [53] I. Michael, L. Rizzo, C.S. McArdell, C.M. Manaia, C. Merlin, T. Schwartz, C. Dagot, D. Fatta-Kassinos, Urban wastewater treatment plants as hotspots for the release of antibiotics in the environment: A review, *Water Res* 47 (2013) 957–995, <https://doi.org/10.1016/j.watres.2012.11.027>.
- [54] N.H. Tran, H. Chen, M. Reinhard, F. Mao, K.Y.-H. Gin, Occurrence and removal of multiple classes of antibiotics and antimicrobial agents in biological wastewater treatment processes, *Water Res* 104 (2016) 461–472, <https://doi.org/10.1016/j.watres.2016.08.040>.
- [55] M. Kocárek, R. Kodesová, L. Vondracková, O. Golovko, M. Fér, A. Klement, A. Nikodem, O. Jaksík, R. Grabic, Simultaneous sorption of four ionizable pharmaceuticals in different horizons of three soil types, *Environ. Pollut.* 218 (2016) 563–573, <https://doi.org/10.1016/j.envpol.2016.07.039>.
- [56] A.A. Aryee, F.M. Mpatani, E. Dovi, Q. Li, J. Wang, R. Han, Z. Li, L. Qu, A novel antibacterial biocomposite based on magnetic peanut husk for the removal of trimethoprim in solution: Adsorption and mechanism study, *J. Clean. Prod.* 329 (2021), 129722, <https://doi.org/10.1016/j.jclepro.2021.129722>.
- [57] C. Monahan, D. Morris, R. Nag, E. Cummins, Risk ranking of macrolide antibiotics – Release levels, resistance formation potential and ecological risk, *Sci. Total Environ.* 859 (2023), 160022, <https://doi.org/10.1016/j.scitotenv.2022.160022>.
- [58] N. Magesh, A.A. Renita, R. Siva, N. Harirajan, A. Santhosh, Adsorption behavior of fluoroquinolone(ciprofloxacin) using zinc oxide impregnated activated carbon prepared from jack fruit peel: Kinetics and isotherm studies, *Chemosphere* 290 (2022), 133227, <https://doi.org/10.1016/j.chemosphere.2021.133227>.